Smart dynamic rotor control: Part 3, advanced controller design.

Jan-Willem van Wingerden
j.w.vanwingerden@tudelft.nl

Teun Hulskamp
a.w.hulskamp@tudelft.nl

Thanasis Barlas
a.barlas@tudelft.nl

Ivo Houtzager
i.houtzager@tudelft.nl

Harald Bersee
h.e.n.bersee@tudelft.nl

Gijs van Kuik
g.a.m.vankuik@tudelft.nl

Michel Verhaegen
m.verhaegen@tudelft.nl

DUWIND, Delft University of Technology, Delft, The Netherlands

Abstract

In this paper, which is a part of a three-part series, a proof of concept study is performed to show the feasibility of the load alleviation abilities of a 'Smart' rotor; that is, a rotor where the blades are equipped with a number of control devices that locally change the lift profile on the blade, combined with appropriate sensors and feedback controllers. This research is performed with on scaled 2-bladed turbine at the new 3 m Ø open jet wind tunnel facility of the Delft University of Technology.

With this paper being part of a three-part series, where in part one the structural dynamics and design is explained and in part II the aerodynamics and the first principles modeling are discussed, we address in this part the controller design. The proposed main contribution of this paper is then twofold: first we bring the feasibility studies performed so far to a higher level by looking at a flexible two-bladed rotating 'smart' rotor. Second, we show the potential and the need for modern control techniques for the 'smart' rotor by enabling both advanced feedback and feedforward control. For controller synthesis we use dedicated system identification methods to obtain a dynamic model of the 2-bladed 'smart' rotor of which each blade is equipped with trailing edge flaps and strain sensors to facilitate feedback control. A feedback controller based on $\mathcal{H}_\infty$ loop shaping combined with a fixed-structure feedforward is designed that minimizes the root bending moment in the flapping direction of the two blades. We show that with appropriate control techniques the loads, variations in the blade root moments, can be reduced up to 88%.

Keywords: 'smart' rotor, system identification, feedback control, feedforward control

1 Introduction

There have been two main operation concepts to keep the loads on wind turbines (*e.g.* fatigue loads, power variations) within acceptable limits and to optimize the energy yield. The concept widely used from the seventies until the nineties of the previous century was the 'Danish concept' [1]. Such turbines combine constant rotor speed with stall of the flow around the rotor blades and are stable by design; increasing wind speeds automatically induce increasing drag forces that limit the produced power (this concept is also referred to as: stall control turbine). In that period, all other control options were considered too complex and also the technology for variable speed control was not mature enough. Due to the development of dedicated converters, regulation concerning maximum allowable sound emissions and grid requirements, the most recent large wind turbines run at variable rotational speed, combined with the adjustment of the collective pitch angle of the blades [2].

Full-span collective pitch control, as previously discussed, is widely accepted in the wind energy community, but can only handle slow wind changes that affect the entire rotor. Because of the increasing rotor size it is necessary to react to the distributed nature of turbulence in a more detailed way: each blade separately and at several separate radial distances. This first item is dealt with by Individual Pitch Control (IPC) [3, 4, 5], motivated by the helicopter industry [6], which is the latest development in the wind turbine industry to further minimize the loads and is ready to be commercialized. With this concept each blade is pitched individually to suppress the periodic loads caused by tower shadow, wind shear, rotational sampling, yaw misalignment, etc. However, the performance of the IPC method is restricted by the limited bandwidth of and wear in the pitch actuators and because they only affect the load on the whole blade. A more advanced operation concept is required to further reduce the loads in order to optimize the rotor diameter with respect to weight and size.

One advanced operation concept is to use a number of actuators that locally change the force profile on the wind turbine blade to cope with the spatial distributed nature of turbulence. This, in combination with sensors that measure the loads and a controller that manipulates the measured signals and generates an appropriate actuation signal, is defined as the 'smart' rotor concept (for more concepts see [7]).

The main goal of the 'smart' rotor is to reduce the fatigue loads to increase the lifetime of the wind turbine. However, when the lifetime constraint is reached the wind turbine rotor size may be increased or the rotor design may be optimized with respect to weight. Recently some research on this topic has been performed in the wind industry where trailing edge flaps [8, 9, 10], and MEM-tabs [11, 12] have been used for load alleviation.

The first experimental feasibility study that takes the blade aeroelastic effects and a feedback Single-Input Single-Output (SISO) controller into account, thus proving the concept of a 'smart' rotor blade, is given in [13] on a non-rotating experiment. In this three-part series we are making the next step towards a rotating feasibility step and in particular in this paper we look at more advanced controller designs to cope with the inherent Multiple-Input Multiple-Output nature of the 'smart' rotor concept.

The outline of this paper is as follows: In Section 2 we briefly introduce the experimental setup. In Section 3 and 4 we propose the control architecture for the feedback and feedforward path, respectively. The performance of the combined controller and combinations thereof are presented in Section 5. We finalize this paper with a number of conclusions and recommendations.

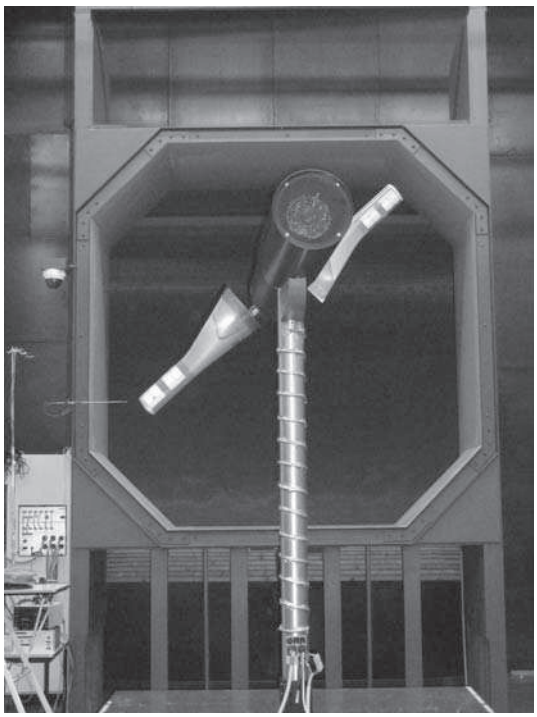

Figure 1: Experimental setup

2 Experimental setup

In this section we briefly present the experimental setup used to show the feasibility of the 'smart' rotor concept for more details we refer to Part I of this three-part series. The 'smart' rotor that we use for our experimental validation is a rotating, two-bladed rotor equipped with trailing-edge flaps. An indication of the size and the lay-out of the turbine can be found in Fig. 1. Each blade is equipped with two distinct trailing-edge flaps to enable its use for future research. Since, for this study the main focus is to suppress the bending behavior of the two individual blades, the two actuators on one blade are used together as one actuator by applying the same control signal. For the same reason two strain sensors are applied in the root located on the central axis and at the leading edge of the blade, respectively. The experimental setup mainly consists of the following components:

Wind tunnel

The experiments are conducted in the Delft University of Technology's Open Jet Facility (OJF) wind tunnel.

Blade Design

The blade was dynamically scaled such that the ratio between the rotational speed and the blade's first eigenmode was the same as with the reference design, the UpWind 5 MW wind turbine. For more details please look at Part I of this three-part series.

Actuators & sensors

Every blade was equipped with two trailing-edge flaps in the outboard part of the blade, which is where the largest aerodynamic leverage can be obtained.

For control purposes, the blade is equipped with sensors which measure the dynamic behavior of the blade. Because the final goal for this rotating 'smart' rotor is to reduce the fatigue loads, two Macro Fiber Composite (MFC) patches are adhered to the root to measure the high strains associated with the first flapwise bending mode.

Real-Time environment

The control intelligence and data acquisition capability are added with the inclusion of a dSPACE$^{\mathrm{tm}}$ chip. The controller and data acquisition scheme are fully developed in the Matlab$^{\mathrm{tm}}$ and Simulink$^{\mathrm{tm}}$ environment and then compiled to the dSPACE$^{\mathrm{tm}}$ chip. On a separate computer all the signals are monitored using Control Desk$^{\mathrm{tm}}$ and the control parameters can be adjusted real-time in the same environment.

3 Feedback design

For controller design it is important to know the dynamic relation between the actuators used for control, the control device, and the sensors used for control. Obtaining this model is outside the scope of this paper but experimental or first-principles modeling can be used to obtain a model for control. Similar as in [13] we follow the data-driven approach to obtain a model from measurement data (using system identification) which is an emerging discipline for wind turbine control research. Since we

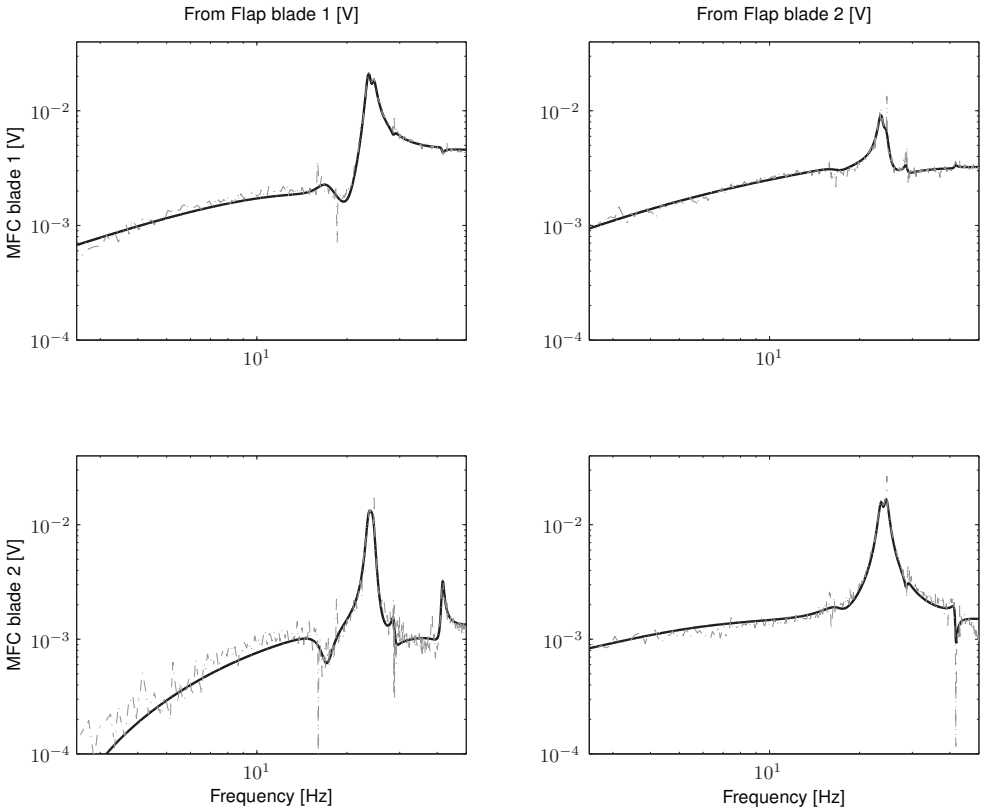

Figure 2: The model used for controller design is given by means of a Bode magnitude plot. The solid line is the identified model while the dashed line represents the frequency response estimate.

have to cope with extremely dominant periodic disturbances (1P, 2P and 3P) we use the method proposed in [14] to estimate the model and for more details we refer to this particular paper. The estimated model in presented in Fig. 2 since it contains crucial information for controller synthesis. It is given by means of a Bode plot since in industry it is common practice to use such a Bode magnitude plot to graphically understand and evaluated the tuning process. From Fig. 2 there are basically two observations which are of interest. First we see a strong coupling between the different actuators and sensors and second the system is not symmetric. The first observation motivates the use of MIMO control. Although one can consider decoupling of the different feedback loops this becomes more and more difficult when there are multiple flaps active on one blade and that is why we use MIMO control. The second observation shows the strength of the data-driven approach since the different uncertainties (center of gravity, different connections, flap deflection) can be different for the two blades. By performing a system identification experiment these uncertainties are directly visible and the controller can take this asymmetric dynamics into account.

The goal of feedback control is to suppress the unknown disturbances as much as possible; however, the ability to do so is limited by the requirement that the system should remain stable. For SISO stable non-minimum phase system, manual loop-shaping is a well known method to design stable feedback controllers based on the Bode plot of the system of interest. For MIMO systems manual loopshaping becomes rather complicated

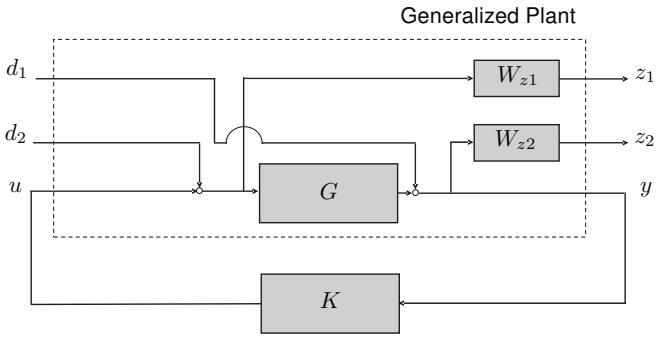

Figure 3: Illustration of the generalized plant used to synthesize the four block $\mathcal{H}_\infty$ controller.

and that is why we use the $\mathcal{H}_\infty$ controller design framework. We use the so-called four block $\mathcal{H}_\infty$ control synthesize setting [15]. In this setting it is common to visualize the control problem in the generalized plant setting, which is shown in Fig. 3 (see also [16]). The $\mathcal{H}_\infty$ controller will minimize the $\mathcal{H}_\infty$ norm between d_1, d_2 (disturbance signals) and z_1, z_2 (performance signals), and this is mathematically given by:

$$\left\| \begin{bmatrix} W_{z1}K\left(I-GK\right)^{-1} & W_{z1}\left(I-KG\right)^{-1} \\ W_{z2}\left(I-GK\right)^{-1} & W_{z2}\left(I-GK\right)^{-1}G \end{bmatrix} \right\|_\infty .$$

In the controller design cycle we can embed the manual loop shaping ideas in the weighting filters W_{z1} and W_{z2}.

We choose W_{z2} in such a way that we penalize the 1-3P frequencies (or a selection thereof) by including inverted notches at these frequencies and we also add a

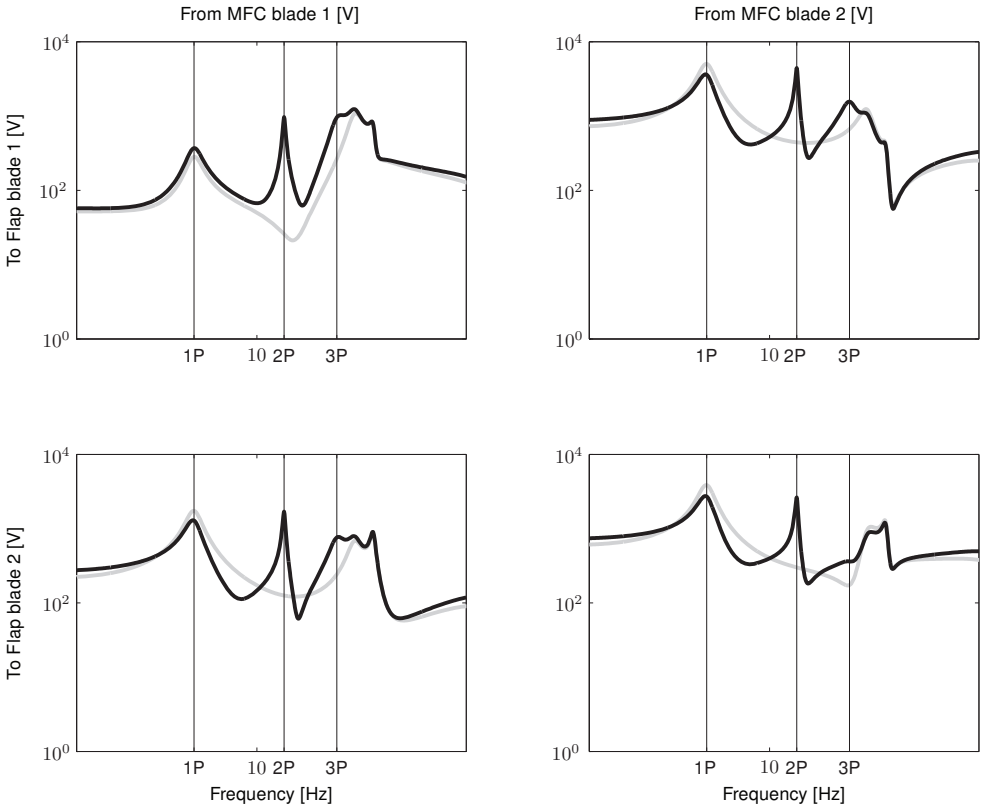

Figure 4: Two different feedback controllers are depicted by means of their Bode magnitude plot where the grey line corresponds with the controller that targets the $1P$ disturbance and the first flapping mode and the black line has the some objectives but with additional load reduction capabilities at the $2P$ and $3P$ frequency.

notch at the first flapping mode to obtain damping enhancement. We choose W_{z1} in such a way that the controller will not act on high frequencies by weighting the controller sensitivity by a filter with high gains at high frequencies. In this paper we compare two designs. For the first controller we add an inverted notch at the 1P and the first natural frequency in the weighting filter W_{z2}. The second filter is completely the same but additional notches are added at the $2P$ and $3P$. The two different controllers are given in Fig. 4 where we clearly can make a distinction between the two feedback controllers. In the experimental section we will compare the two feedback controllers and we will add an feedforward controller to the system which is the topic of the next section.

4 Feedforward design

Since we know the shapes and frequencies of the most dominant deterministic disturbances we can embed them in a feedforward signal. However, we do not know the phase and amplitude necessary to compensate for the disturbances. To do so we have to learn these properties. These properties can be linearly parameterized by defining the following fixed-structure feedforward signal:

$$u_k^{(ff)} = \sum_{i=1}^{q} \theta_i^s sin(i\omega t) + \theta_i^c cos(i\omega t)$$

where t is time in s and ω the rotational speed in rad/s. Further, we have the unknowns θ_i^s and $\theta_i^c \in \mathbb{R}^r$ and q

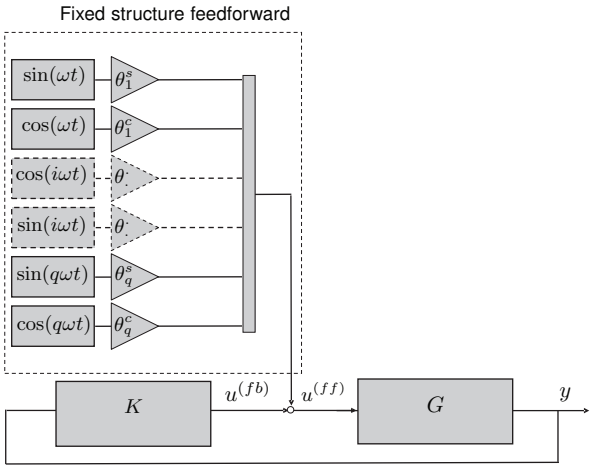

Figure 5: Illustration of the fixed-structure feedforward scheme in combination with feedback.

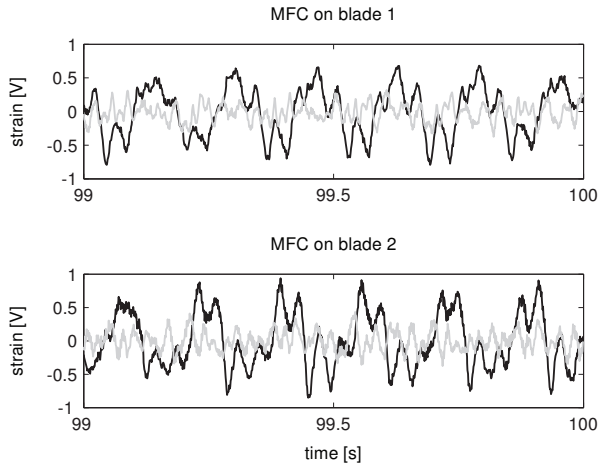

Figure 6: Time domain performance of the controller evaluated on the MFC signal on blade one and two. The grey line is with $\mathcal{H}_\infty$ feedback targeting the 1P, 2P, 3P and first natural frequency and fixed-structure feedforward control and the black one is without any control. For V=7 m/s and $\omega = 370$ RPM.

the number of periodic components that should be taken into account. The fixed-structure feedforward scheme is illustrated in Fig. 5. The question appears how do we select these θ's? We use ideas from repetitive control to learn these parameters but we will not elaborate on that in this paper and we refer to [17] where a data-driven approach is developed to adaptively learn the unknowns. However, is the experimental results we can clearly see the benefits of the chosen approach when we combine this feedforward scheme with feedback.

5 Experimental results

In this section we present the results of the two different feedback controllers combined with the feedforward scheme for one operational condition. This operational condition is characterized by a wind speed of 7 m/s and a rotational speed of 370 RPM. We have a stochastic perturbations coming from the wind (turbulence) and periodic mainly deterministic perturbations due to the unbalance of the two-bladed rotor. The results are presented using three graphs (all the results are based on measurements with a length of 2 minutes). In Fig.6 the time domain performance of the advanced controller is given. In this figure the signal is given with (black) and without (grey) controller. For this result we combined the feedforward controller with the $\mathcal{H}_\infty$ controller that targets the 1P, 2P, 3P and the first flapping frequency which was given in Fig. 2. By just looking at the signals a strong vibration reduction can be observed. We will quantify the performance of the different feedback controllers with and without feedforward by looking at the variance of the signals and compare that with the baseline situation where no controller is active. We define this performance measure as follows:

$$\text{Performance} = 100 \times \left(1 - \frac{\text{var(y)}}{\text{var}(\text{y}_{\text{baseline}})}\right),$$

where y represents the load signal (the MFC signals) and $var(.)$ represents the variance. The results are given in Table 1. In this table we see the positive effect of the feedforward signal. It is hard to make a good distinction between the two different feedback controller. To highlight the effect of the different feedback controllers we plotted the square-root of the smoothed power spectral density with and without the synthesized feedback controller and fixed-structure feedforward controller for the most dominant frequencies, see Fig. 7. The most important observation is that with the feedback controller that only targets the 1P and first flapping mode the 2P frequency is amplified. Although, the result with a feedback controller that only targets the first flapping frequency is not included in this paper, the results showed a significant damping enhancement of the first flapping mode but the other periodic disturbance where amplified. For the controller that targets the whole spectrum of disturbance frequencies we see, as expected, a clear performance improvement at all the periodic multiples of the rotor speed.

6 Conclusions

In this paper a proof of concept study was performed that showed the feasibility of the load alleviation abilities of a 2-bladed rotating 'smart' rotor with special attention for the controller synthesis. A feedback controller based on $\mathcal{H}_\infty$ loop shaping was designed and we proposed to use a fixed-structure feedforward scheme. We evaluated the performance using a number of different load scenario's. We showed that with appropriate control techniques the loads can be reduced up to 88% for nominal operation.

References

[1] J.F. Manwell, J.G. McGowan, and A.L. Rogers. *Wind energy explained; Theory, design and application*. John Wiley and Sons, Ltd, Chichester, 2002.

[2] E.A. Bossanyi. The design of closed loop controllers for wind turbines. *Wind Energy*, 3(3):149–163, 2000.

[3] E.A. Bossanyi. Individual blade pitch control for load reduction. *Wind Energy*, 6(2):119–128, 2003.

[4] E.A. Bossanyi. Further load reductions with individual pitch control. *Wind Energy*, 8(4):481–485, 2005.

[5] K. Selvam, S. Kanev, J. W. van Wingerden, T. van Engelen, and M. Verhaegen. Feedback-feedforward individual pitch control for wind turbine load reduction. *International Journal of Robust and Nonlinear Control,* special issue on Wind turbines: New challenges and advanced control solutions, 19(1):72–91, 2009.

[6] P.P. Friedmann and T. A. Millott. Vibration reduction in rotorcraft using active control: A comparison of various approaches. *Journal of Guidance, Control, and Dynamics*, 18(4):664–673, 1995.

Table 1: The variance of the MFC signals for different control scenarios. In the last two rows the variance reduction is expressed in a percentage of the nominal case (without advanced control).

FeedBack (FB)				FeedForward (FF)	Performance			
damping	1P	2P	3P		MFC blade 1	MFC blade 2	[%]	[%]
-	-	-	-	-	0.151	0.207	-	-
✓	✓	-	-	-	0.047	0.044	69	79
✓	✓	✓	✓	-	0.058	0.029	62	86
-	-	-	-	✓	0.085	0.134	43	35
✓	✓	-	-	✓	0.025	0.020	83	90
✓	✓	✓	✓	✓	0.018	0.024	88	88

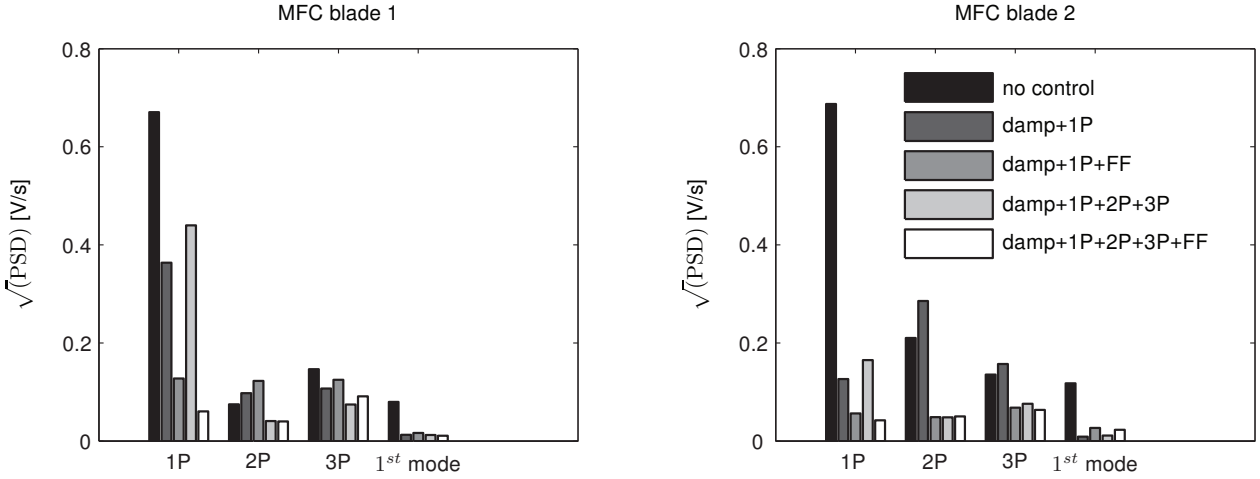

Figure 7: Square-root of the PSD of the MFC signal on blade one and two where only the most dominant disturbances are given. The figure shows the difference between the different controllers. The results are valid for V=7 m/s and $\omega = 370$ RPM.

[7] T. K. Barlas and G. A. M. van Kuik. Review of state of the art in smart rotor control research for wind turbines. *Progress in Aerospace sciences*, 46(1):1–27, 2010.

[8] T. Buhl, M. Gaunaa, and C. Bak. Potential of load reduction using airfoils with variable trailing edge geometry. *Journal of Solar Energy Engineering*, 127(4):503–516, 2005.

[9] P. B. Andersen, L. Henriksen, M. Gaunaa, C. Bak, and T. Buhl. Deformable trailing edge flaps for modern megawatt wind turbine controllers using strain gauge sensors. *Wind Energy*, 13(2-3):193–206, 2010.

[10] C. Bak, M. Gaunaa, P. B. Andersen, T. Buhl, P. Hansen, and K. Clemmensen. Wind tunnel test on airfoil risø-b1-18 with an active trailing edge flap. *Wind Energy*, 13(2-3):207–219, 2010.

[11] J.R. Zayas, C. P. van Dam, R. Chow, J.P. Baker, and E.A. Mayda. Active aerodynamic load control for wind turbine blades. In *Proceedings of the European Wind Energy Conference (EWEC)*, Athens, Greece, 2006.

[12] C. P. van Dam, R. Chow, J.R. Zayas, and D. A. Berg. Computational investigations of small deploying tabs and flaps for aerodynamic load control. *Journal of Physics, Conference series: The Science of Making Torque from Wind*, 75(012027), 2007.

[13] J. W. van Wingerden, A.W. Hulskamp, T. Barlas, B. Marrant, G. A. M. Van Kuik, D-P. Molenaar, and M. Verhaegen. On the proof of concept of a 'smart' wind turbine rotor blade for load alleviation. *Wind Energy*, 11(3):265–280, 2008.

[14] G. van der Veen, J.W. van Wingerden, and M. Verhaegen. Closed loop identfication of wind turbines in the presence of periodic effects. In *Proceedings of the 3^{th} conference, The Science of Making Torque from Wind*, 2010.

[15] S. Skogestad and I. Postlethwaite. *Multivariable feedback control, analysis and design*. John Wiley and sons, 1996.

[16] H.M.N.K. Balini, I. Houtzager, J. Witte, and C. W. Scherer. Subspace identification and robust control of an AMB system. In *American Control Conference 2010*, 2010.

[17] J.W. van Wingerden, A.W. Hulskamp, T. Barlas, I. Houtzager, H.E.N. Bersee, G. A. M Van Kuik, and M. Verhaegen. Two-degree-of-freedom active vibration control of a prototyped 'smart' rotor. *submitted to IEEE Transactions on Control System Technologies*, -:–, 2010.